

Effect of H impurity on misfit dislocation in Ni-based single-crystal superalloy: molecular dynamic simulations*

Yu Tao(于涛)^{a)†}, Xie Hong-Xian(谢红献)^{a)c)}, and Wang Chong-Yu(王崇愚)^{a)b)}

^{a)} Central Iron and Steel Research Institute, Beijing 100081, China

^{b)} Department of Physics, Tsinghua University, Beijing 100084, China

^{c)} School of Mechanical Engineering, Hebei University of Technology, Tianjin 300132, China

(Received 27 October 2011; revised manuscript received 17 November 2011)

The effect of H impurity on the misfit dislocation in Ni-based single-crystal superalloy is investigated using the molecular dynamic simulation. It includes the site preferences of H impurity in single crystals Ni and Ni₃Al, the interaction between H impurity and the misfit dislocation and the effect of H impurity on the moving misfit dislocation. The calculated energies and simulation results show that the misfit dislocation attracts H impurity which is located at the γ/γ' interface and Ni₃Al and H impurity on the glide plane can obstruct the glide of misfit dislocation, which is beneficial to improving the mechanical properties of Ni based superalloys.

Keywords: molecular dynamic, H impurity, misfit dislocation, Ni-based superalloy

PACS: 61.72.Lk, 02.70.Ns, 8540.Ry

DOI: 10.1088/1674-1056/21/2/026104

1. Introduction

Nickel-based single-crystal superalloys are widely used for hot section turbine components.^[1,2] The microstructure of the superalloy consists of a high volume of fraction of cuboidal γ' phase (L12 structure) separated by narrow γ channels (face-centered cubic solid solution).^[3] The γ' cuboids generally align along the [100] lattice direction, each of which has an average edge length of the order of 500 nm. Due to the edge length of the γ' cuboidal is very small, there is a vast interfacial region between the solid solution γ phase and the ordered γ' precipitates.^[4] It is believed that the structure and properties of γ/γ' interface greatly affect the shape, the size and the coarsening rate of γ' precipitates, which in turn is a major factor influencing creep rupture strength of superalloy.^[5]

The stability of the γ/γ' interface was studied by several groups. The strengthening effects induced by alloying elements on coherent γ/γ' interface were surveyed by Chen *et al.*^[6] using first-principles quantum mechanics DMol3 calculations and the calculations showed that alloying elements significantly increase the net vertical and horizontal bond-order values, with

Mo yielding the most effective cohesive strength, while W yielding the most effective shear strength. The synergetic effect of Re and Ru on coherent γ/γ' interface strengthening was also investigated by Chen *et al.*^[7] using the same method. The results showed that the synergetic effect of Re and Ru on the interface strengthening was better than that achieved by the individual Re or Ru. The effect of residual internal stresses on the stability of the coherent γ/γ' interface was discussed by Yashiroa *et al.*^[8] using molecular dynamic (MD) simulation. The simulation results suggested that the dislocation could derive from the interface.

The difference in lattice parameter between the γ matrix and coherent γ' precipitates creates a very high misfit stress.^[9,10] Obviously, the interface with the stress is unstable. Based on the principle of minimum energy, the atoms in the interface will be rearranged so as to minimize the elastic stress field between γ phase and γ' phase, i.e., a self-accommodating process. Then the network of the interface misfit dislocations will be created and the interphase coherence will be affected. This process shows that the formation of misfit dislocation networks is an important way to

*Project supported by the National Basic Research Program of China (Grant No. 2011CB606402) and the National Natural Science Foundation of China (Grant No. 51071091).

[†]Corresponding author. E-mail: ytao012345@163.com

© 2012 Chinese Physical Society and IOP Publishing Ltd

<http://iopscience.iop.org/cpb> <http://cpb.iphy.ac.cn>

reduce the distorted energy. These misfit dislocations, each of which is edge in character and has a Burgers vector in the plane of the interface, exist in the single crystal superalloy,^[11–13] and have great influence on the mechanical properties of the superalloy.^[14]

Misfit dislocations move in the interface, producing a permanent change of shape. Consequently, how misfit dislocations move in response to stress has been a matter of our serious concern and intensive study. We have studied the motion of misfit dislocation in the γ/γ' interface subjected to applied shear stress.^[15] Our simulation results suggested that the misfit dislocation is easy to slip under the shear stress. A large body of microscopic evidence shows that the presence of H can increase the mobility of dislocation, which results in the localized plasticity. This is called the H-enhanced localized plasticity mechanism.^[16–18] However, to our knowledge, there is neither direct experimental study nor theoretical research on the effect of H impurity on the misfit dislocation in the γ/γ' interface.

In the present work, we make effort to investigate the effect of H on the misfit dislocation using the MD simulation. The embedded-atom-method (EAM) potential for H–Ni–Al system^[19,20] is used for the atomic interaction. The EAM potential is very successful in the study on the H–Ni–Al system.^[21–23] The outline of this work is organized as follows: we present the site preferences of H in Ni and Ni₃Al in Section 2. Section 3 is devoted to the construction of the model of misfit dislocation. The interaction between H impurity with misfit dislocation and the effect of H impurity on the moving misfit dislocation are discussed in Sections 4 and 5, respectively. Finally, the simulation results and main conclusions are summarized in Section 6.

2. Site preferences of H in Ni and Ni₃Al

In order to study the effect of the H impurity on the misfit dislocation, it is necessary to identify the interstitial site that the H impurity prefers to occupy. There are two types of interstitial sites in Ni and three types of interstitial sites in Ni₃Al, respectively (see Fig. 1). The impurity formation energy (IFE) is defined as follows:

$$E_{\text{imp}} = E_{\text{tot}}(\text{Ni}(\text{or Ni}_3\text{Al}) + \text{H}) - E_{\text{tot}}(\text{Ni}(\text{or Ni}_3\text{Al})), \quad (1)$$

where $E_{\text{tot}}(\text{Ni}(\text{or Ni}_3\text{Al}) + \text{H})$ is the total energy of the system with the H impurity lying at a certain interstitial site and $E_{\text{tot}}(\text{Ni}(\text{or Ni}_3\text{Al}))$ is the total energy of the system without the impurity. To calculate the impurity formation energy we consider a system containing 4000 atoms. We first relax the system using MD and calculate the $E_{\text{tot}}(\text{Ni}(\text{or Ni}_3\text{Al}))$, then place the H impurity at a certain interstitial site and relax the system and calculate the $E_{\text{tot}}(\text{Ni}(\text{or Ni}_3\text{Al}) + \text{H})$.

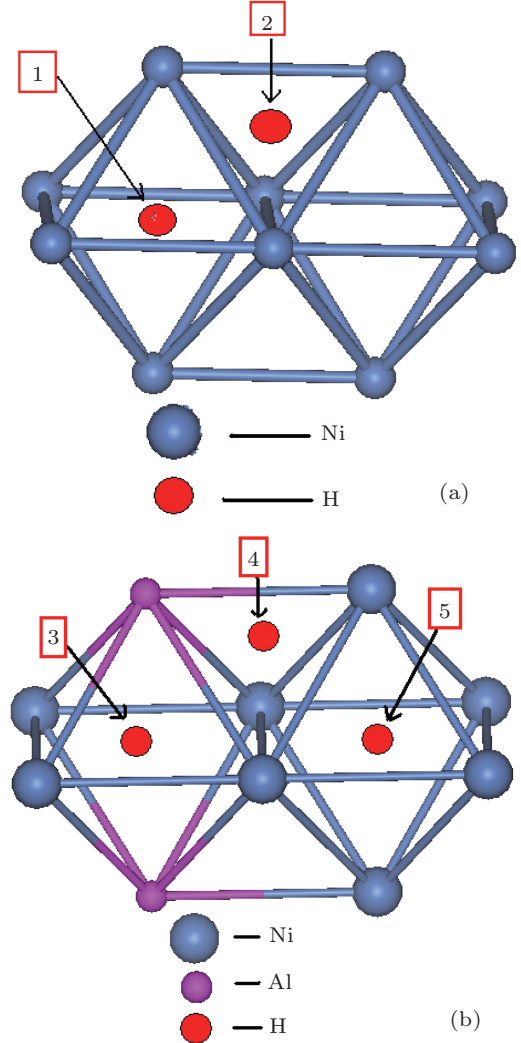


Fig. 1. (colour online) Sites of H impurity in Ni (a) and Ni₃Al (b).

The IFEs of the H impurity at five different types of interstitial sites are listed in Table 1, showing that the IFE varies with the interstitial site type. It can also be found from Table 1 that all the IFEs at the octahedral interstitial sites are much more negative than those at the tetrahedral interstitial sites in Ni and Ni₃Al, respectively. Thus we consider that H impurity is energetically favourable to occupying the octahedral interstitial site rather than the tetrahedral

interstitial site. Furthermore, there are two types of octahedral interstitial sites in Ni_3Al ; one type is surrounded by six Ni atoms and the other type is surrounded by four Ni atoms and two Al atoms. From Table 1 we can consider that H impurity is energetically favourable to occupying the octahedral interstitial site surrounded by six Ni atoms rather than the octahedral interstitial site surrounded by four Ni atoms and two Al atoms. Therefore, the following studies of interaction of H impurity and the misfit dislocation are carried out only when an H atom is located at the octahedral interstitial site in Ni and the octahedral interstitial site surrounded by six Ni atoms in Ni_3Al .

Table 1. Impurity formation energies (in eV) of the H impurity at five different types of interstitial sites.

Interstitial site	1	2	3	4	5
IFE/eV	-2.19	-1.78	-1.71	-1.41	-2.34

3. Construction of the model of misfit dislocation

Both Ni and Ni_3Al possess the face-centred-cubic structure; however the lattice parameters of the two are not identical. When the lattice misfit exceeds the limit of elasticity, the misfit dislocation will be formed in the interface to reduce the distorted energy of the system. Considering the concept of coincidence site lattice in the misfit interface, we can write such a relation^[13,24,25] as

$$(n+1)a_{\text{Ni}} = na_{\text{Ni}_3\text{Al}}, \quad (2)$$

where n is n -fold of the lattice parameter, a_{Ni} and $a_{\text{Ni}_3\text{Al}}$ are the lattice parameters of Ni and Ni_3Al , respectively. In the present work, the lattice parameters of Ni and Ni_3Al are $a_{\text{Ni}} = 0.352$ nm and $a_{\text{Ni}_3\text{Al}} = 0.3573$ nm, respectively, so we can obtain $n = 66$. It indicates that within the range of misfit interface formed by 66 Ni_3Al lattices and 67 Ni lattices, the stress induced by the difference of lattice parameters should be relaxed.

According to the above analysis, we can construct the misfit dislocation model (see Fig. 2). The simulation model with (010) interface that is oriented along the axes $x = [101]$, $y = [10\bar{1}]$, and $z = [010]$ is divided into the two parts by the (010) plane, including a total of 778360 atoms. The upper part is Ni, with box vectors $67[101]$, $67[10\bar{1}]$, and $11[010]$, respectively; and the lower parts is Ni_3Al , with box vectors $66[101]$, $66[10\bar{1}]$, and $11[010]$, respectively. The model is periodic along the x and the y directions and has free surfaces as upper and lower boundaries in the z direction.

Through the MD relaxation at $T = 0$ K we can obtain the equilibrium atomic structure of dislocation in the γ/γ' interface. According to the potential energy of atoms, we select the atoms with the higher potential energies in the dislocation core area and along the dislocation line. The pattern of the misfit dislocation in the (010) γ/γ' interface is shown in Fig. 3. These misfit dislocations are edges in character and the slip plane of them is the (010) interface. The index of the misfit dislocations can be written as $\langle 011 \rangle \{100\}$.^[13]

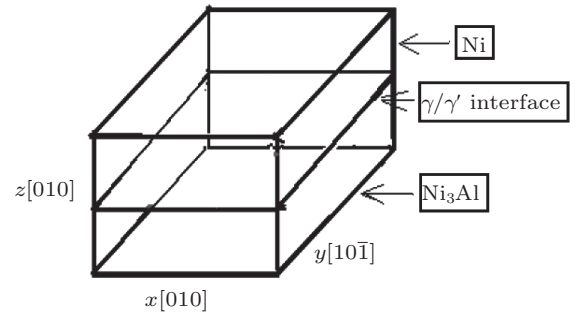


Fig. 2. Diagrammatic sketch of the initial model.

4. Interaction between H impurity and misfit dislocation

In this section, we study the interaction between H impurity and misfit dislocation. An H atom is inserted near the misfit dislocation area (see Fig. 3). Because the H impurity is far enough from the other three misfit dislocations, we can consider that the H impurity interacts only with the misfit dislocation nearby. Considering that the γ/γ' interface only has one type of octahedral interstitial site which is surrounded by four Ni atoms and two Al atoms, we locate the H atom at this type of octahedral interstitial site (see Fig. 4).

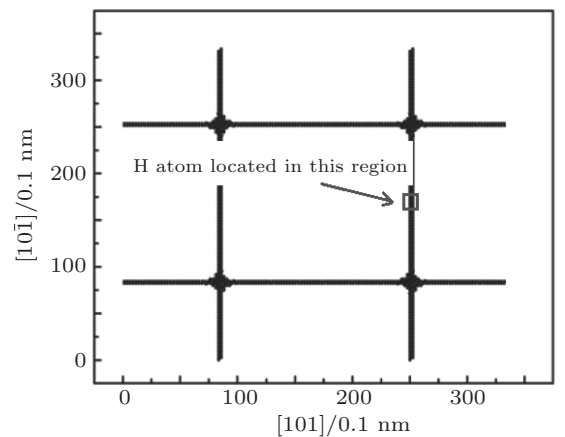


Fig. 3. Pattern of the misfit dislocation in the γ/γ' interface.

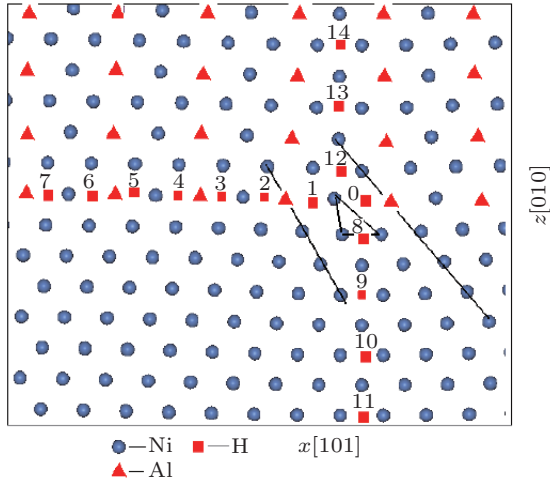


Fig. 4. (colour online) Sites of H impurity near the misfit dislocation.

After locating the H impurity at a certain octahedral interstitial site, we relax the system using MD at $T = 0$ K and calculate the total energy of the system. The total energies of the system at different interstitial

sites are listed in Table 2. It can be found from Table 2 that the total energy of the system increases with the increase of the distance from the misfit dislocation core to the H impurity which is located at the γ/γ' interface and this indicates that the misfit dislocation can attract the H impurity which is located at the γ/γ' interface. When the H impurity is located at site 8, the total energy of the system is -3488049.52 eV; when the H impurity is located at site 11, the total energy of the system is -3488049.69 eV; the total energy of the system decreases with the increase of the distance from the misfit dislocation core to the H impurity that is located at Ni. On the contrary, the total energy of the system increases with the increase of the distance from the misfit dislocation core to the H impurity that is located at Ni_3Al . This reveals that the misfit dislocation can attract the H impurity that is located at Ni_3Al but repel the H impurity that is located at Ni.

Table 2. Total energies (in eV) of the system with the impurity H lying at certain octahedral sites.

Octahedral site	Total energies of the system/eV	Octahedral site	Total energies of the system/eV
0	-3488049.85	8	-3488049.52
1	-3488049.66	9	-3488049.60
2	-3488049.36	10	-3488049.66
3	-3488049.26	11	-3488049.69
4	-3488049.23	12	-3488050.05
5	-3488049.21	13	-3488049.98
6	-3488049.21	14	-3488049.94
7	-3488049.20		

5. Effect of H on the moving misfit dislocation

In this section we discuss a gliding misfit dislocation encountering an H impurity in its glide plane. An H impurity is inserted in octahedral site 3 (see Fig. 4) and the simulation model is shown in Fig. 5. The model is periodic along the x and the y directions and has free surfaces as upper and lower bounds in the z direction. Then the system is relaxed at $T = 300$ K. During the relaxation, the lattice parameters are adjusted to maintain zero pressure in the system. To entice the misfit dislocation to move, shear stress $\tau_{zx} = 251$ MPa is applied through forces on several atomic layers at the free surfaces. Simulations are carried out by integrating Newton's equations of motion^[26] for all atoms using a time step of 0.4 fs.

The temperature of the system keeps 300 K during the loading process, which is obtained by scaling the

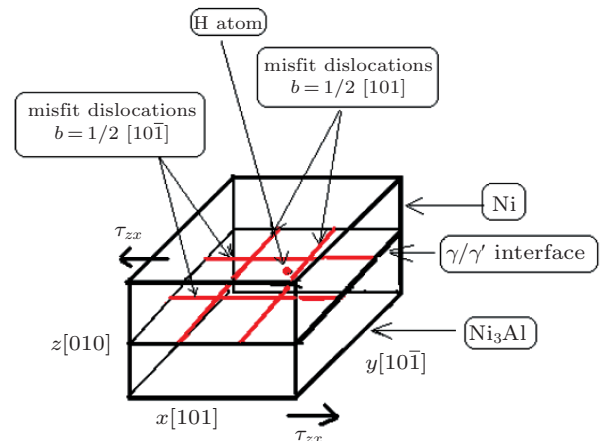


Fig. 5. (colour online) View of MD simulation box used in the calculations.

instantaneous velocities of all atoms with an appropriate Maxwell–Boltzmann distribution at a specified temperature.

Figure 6 shows a series of images of the gliding misfit dislocation encountering an H impurity in its glide plane. At 2.4 ps the double kinks are formed on the misfit dislocation and then migrate along the misfit dislocation lines; the migration of the double kinks leads to the motion of the misfit dislocation. By the time of 2.8 ps most of the misfit dislocations arrive at the place just below the H impurity. Then the most of misfit dislocations go over the H impurity at 3.6 ps, by the time of 4.0 ps the whole misfit dislocation arrives at the place just above the H impurity. At 4.8 ps the double kinks are formed and migrate along the misfit dislocation lines; at 5.2 ps only part of misfit dislocations near the H impurity lag behind the other part of the misfit dislocations; by the time of 6.0 ps the misfit dislocation glides forward and separates from the H impurity. The simulation results indicate that the H impurity in the glide plane can obstruct the glide of misfit dislocation, which is beneficial to improving the mechanical properties of Ni-based superalloys.

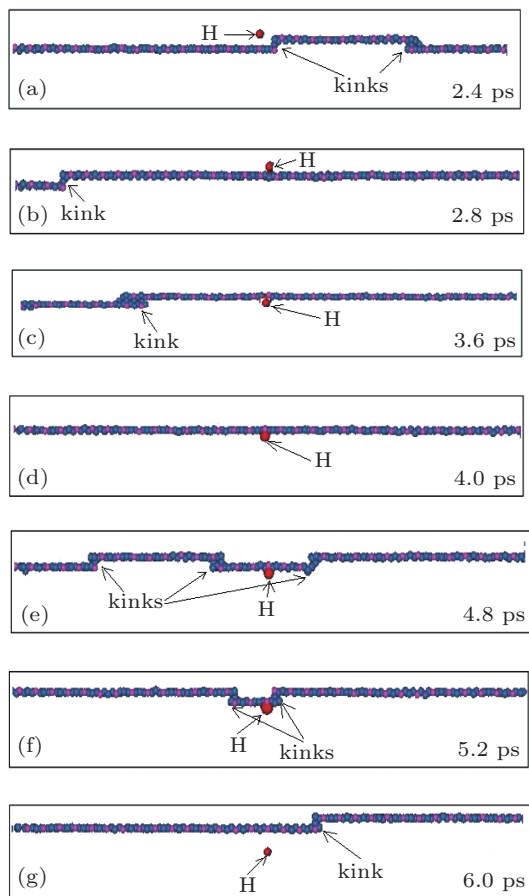


Fig. 6. (colour online) Effect of H on the moving misfit dislocations (visualized by atoms in the misfit dislocation core) at $T = 300$ K and $\tau_{zx} = 251$ MPa.

To study the motion of the H impurity, the x coordinate of H impurity is recorded every 20 fs during the simulation. Because the misfit dislocation glides along the x direction, figure 7 only gives the x coordinate of the H impurity during the simulation process. At the beginning of the simulation, the x coordinates of H impurity and misfit dislocation are 24.49 nm and 25.12 nm, respectively. Before 1.2 ps the H impurity oscillates near the 24.49 nm; this is because that the interaction between the H impurity and the misfit dislocation is too weak to attract the H impurity moving toward the misfit dislocation. After 1.2 ps the distance between the H impurity and misfit dislocation is short enough for attracting the H impurity moving toward the misfit dislocation. By the time of 2.8 ps, the H impurity and misfit dislocation meet with each other, then the H impurity moves with the misfit dislocation for about 3.7 ps. When the simulation time is 6.5 ps, the H impurity stops moving with the misfit dislocation and oscillates near the equilibrium position. In our simulation the Portevin–le Chatelier effect (the solute atoms diffuse with the moving dislocation) does not occur, this is probably because the temperature of our model is low and the applied shear stress is high, the H impurity is not able to achieve a velocity with the same order as the dislocation velocity.

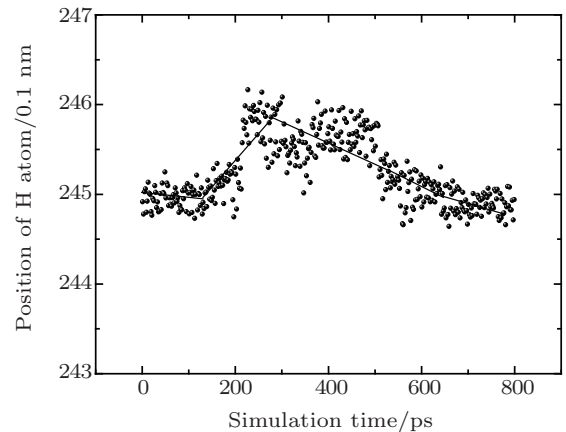


Fig. 7. Valuation of H atom position with time in the simulation process.

6. Summary

In the present work, the effect of H impurity on the misfit dislocation in Ni-based single-crystal superalloy is investigated using the MD simulation. The embedded-atom-method (EAM) potential for H–Ni–Al system is used for the atomic interaction. We first study the site preferences of H impurity in single crystals Ni and Ni₃Al and find that the H impurity is

energetically favourable to occupying the octahedral interstitial site in Ni and occupying the octahedral interstitial site surrounded by six Ni atoms rather than the octahedral interstitial site surrounded by four Ni atoms and two Al atoms in Ni₃Al. Then the model of misfit dislocation is constructed and the interaction between H impurity and the misfit dislocation is investigated. The calculated results indicate that the misfit dislocation attracts the H impurity which is located at the γ/γ' interface and Ni₃Al; on the contrary, the misfit dislocation repels the H impurity which is located at Ni. Finally, the effect of H impurity on the moving misfit dislocation is also discussed and the simulation results show that the H impurity in the glide plane can obstruct the glide of misfit dislocation, which is beneficial to improving the mechanical properties of Ni-based superalloys.

References

- [1] Ross E W and Sims C T 1987 "Nickel-Base Alloys", in: Sims C T, Stoloff N S and Hagel W C eds. *Superalloy II* (High Temperature Materials for Aerospace and Industrial Power) (New York: John Wiley & Sons) p. 97
- [2] Pollock T M and Argon A S 1992 *Acta Metall. Mater.* **40** 1
- [3] Nabarro F R N and Villiers H L 1995 *The Physics of Creep* (London: Taylor & Francis)
- [4] Anton D L in: Westbrook J H and Fleischer R L eds. 1994 *Intermetallic Compounds* (New York: Wiley) **2** 3
- [5] Mirkin I L and Kancheev O D 1967 *Met. Sci. Heat Treat.* **1-2** 10
- [6] Chen K, Zhao L R and John S Tse 2004 *Mater. Sci. Eng. A* **365** 80
- [7] Chen K, Zhao L R and John S Tse 2003 *Mater. Sci. Eng. A* **360** 197
- [8] Yashiro K, Naitob M and Tomitac Y 2002 *Int. J. Mech. Sci.* **44** 1845
- [9] Pollock T M and Argon A S 1992 *Acta Metall. Mater.* **40** 1
- [10] Socrate S and Parks D M 1993 *Acta Metall. Mater.* **41** 2185
- [11] Lahrman D F, Field R D, Darolia R D and Fraser H L 1988 *Acta Metal.* **36** 1309
- [12] Gabb T P, Draper S L, Hull D R and Nathal M V 1989 *Mater. Sci. Eng. A* **118** 59
- [13] Zhu T and Wang C Y 2005 *Phys. Rev. B* **72** 014111
- [14] Zhang J X, Murakumo T, Koizumi Y, Kobayashi T and Harada H 2003 *Acta Mater.* **51** 5073
- [15] Xie H X, Wang C Y and Yu T 2009 *Modelling Simul. Mater. Sci. Eng.* **17** 055007
- [16] Beachem C D 1972 *Metall. Trans.* **3** 437
- [17] Lynch S P 1988 *Acta Metall.* **36** 2639
- [18] Birnbaum H K and Sofronis P 1994 *Mater. Sci. Eng. A* **176** 191
- [19] Angelo J E, Moody N R and Baskes M I 1995 *Modelling Simul. Mater. Sci. Eng.* **3** 289
- [20] Baskes M I, Sha X, Angelo J E and Moody N R 1997 *Modelling Simul. Mater. Sci. Eng.* **5** 651
- [21] Baskes M I, Angelo J E and Moody N R in: Thompson A W and Moody N R eds. 1996 *Hydrogen Effects in Materials* (Warrendale, PA: The Minerals, Metals and Materials Society) p. 77
- [22] Wen M, Fukuyama S and Yokogawa K 2004 *Phys. Rev. B* **69** 174108
- [23] Wen M, Fukuyama S and Yokogawa K 2007 *Phys. Rev. B* **75** 144110
- [24] Zhu T, Wang C Y and Gan Y 2009 *Acta Phys. Sin.* **58** 156 (in Chinese)
- [25] Xie H X, Yu T and Liu B 2011 *Acta Phy. Sin.* **60** 046104 (in Chinese)
- [26] Allen M P and Tildesley D J 1987 *Computer Simulation of Liquids* (New York: Oxford University Press) p. 83